Journal of Alloys and Compounds 323–324 (2001) 851–854

Journal of ALLOYS AND COMPOUNDS

www.elsevier.com/locate/jallcom

Optical characterisation of rare earths in natural fluorapatite

E. Cantelar[a,*], G. Lifante[a], T. Calderón[b], R. Meléndrez[c], A. Millán[b], M.A. Alvarez[d], M. Barboza-Flores[c]

[a]Departamento de Física de Materiales, C-IV, Universidad Autónoma de Madrid, 28049 Madrid, Spain
[b]Departamento de Química Agrícola-Geología-Geoquímica, Universidad Autónoma de Madrid, 28049 Madrid, Spain
[c]Centro de Investigaciones en Física, Universidad de Sonora, Hermosillo, Mexico
[d]Departamento de Cristalografía, Mineralogía y Química Agrícola, Facultad de Química, Universidad de Sevilla, Sevilla, Spain

Abstract

Fluorapatite coming from Jumilla (Spain) has been investigated by means of optical absorption, photoluminescence and lifetimes. The absorption spectra at room and low temperature in the range 450–850 nm showed mainly the presence of Nd^{3+} ions. The emission and excitation spectra in the UV region reveal also the presence of Ce^{3+} ions, which cannot be detected by absorption due to the tail of the matrix absorption edge. In addition to the infrared emission at 0.89, 1.06 and 1.33 μm coming from the Nd^{3+} ions and the UV emission around 380 nm due to the presence of Ce^{3+} ions, an intense red emission ($\lambda=600$ nm) is observed after blue–green excitation. Following the characteristics of the red band as well as its lifetime ($\tau=132$ μs) this emission has been attributed to the presence of Pr^{3+} ions. © 2001 Published by Elsevier Science B.V.

Keywords: Fluorapatite; Semi-precious mineral; Luminescence; Rare earth; Energy transfer

1. Introduction

Apatites are natural semi-precious minerals which can be found in carbonatites and alkaline rocks, being important sources for phosphates. In addition, apatites usually contain a high amount of impurities, particularly rare earths. The general formula of a fluorapatite can be represented by: $A_{10}(MO_4)_6X_2$ where A is a divalent cation (Ca^{2+}, Sr^{2+}, Ba^{2+}), M can be P, As or V, and X represents F^-, Cl^- or even OH^-. The lattice of the fluorapatites can accommodate very easily rare earths by substitution of divalent cation or anion sites, creating a local charge increase, following several reactions [1].

In relation with the impurity detection in fluorapatites, luminescence techniques have been proposed as alternative methods for estimating the distribution and nature of the rare earths incorporated in these minerals [2]. These techniques are based in the fact that most of the natural apatites generate strong luminescence in the UV-VIS-IR spectral regions when they are exposed to UV, laser radiation or electronic excitation [3]. The observed emissions in these minerals have been related to the presence of several impurities in the lattice, which act as activators or emitters such as Ce^{3+}, Eu^{2+}, Eu^{3+}, Dy^{3+}, . . . etc. The luminescent response of these activators is so efficient that impurity concentration less than 100 ppm in even small samples can be easily detected.

In the present work, the study and characterisation of luminescent impurities by optical spectroscopy (absorption and photoluminescence) in natural fluorapatites have been carried out. Several rare earths (Ce^{3+}, Pr^{3+} and Nd^{3+}) have been clearly detected, which besides the UV absorption tail, are responsible for the green–yellow colour of the samples. The lifetime measurements indicate the presence of an efficient energy transfer mechanism that can affect the de-excitation channels associated to the Pr^{3+} and Nd^{3+} ions.

2. Experimental procedure

The natural fluorapatites investigated in this work come from the deposits of La Celia near Jumilla in Murcia (Spain). These natural crystals present a green–yellow characteristic colour. The samples used in this work showed their natural faces very clean and free of defects and therefore, for optical measurements, it was not necessary to cut or polish them.

---

*Corresponding author.

PII: S0925-8388(01)01159-8

Absorption spectra at liquid helium temperature were recorded with a Hitachi spectrophotometer, model U-3501, using a CTI-Cryogenics close-cycle helium cryostat, the sample being positioned orthoaxially with respect to the light probe.

The photoluminescence measurements in the ultraviolet spectral region have been performed using a Jovin Yvon spectrofluorimeter. An Ar$^+$ pumped titanium:sapphire laser (both from Spectra Physics, models 2040E and 3900, respectively) and a Spectra Physics optical parameter oscillator (model MOPO-730) have been used as excitation sources in the visible and near infrared spectral regions. The fluorescence was dispersed by an ARC monochromator model SpectraPro 500-i. In all the luminescent spectra the excitation was orthoaxial and the recorded fluorescence was unpolarised. For lifetime measurements, the signal was averaged and synchronously detected by a digital oscilloscope.

3. Results and discussion

Fig. 1 shows the absorption spectra, at liquid helium temperature, in the 420–840 nm spectral range. As it can be appreciated these natural fluorapatites present a broad transparent window in the visible region, in which it is possible to detect some additional absorption bands which indicate the presence of impurities in the crystal lattice. Their narrow shapes are typical of the electronic transitions between the 4f orbitals of trivalent rare-earth ions. In particular the absorption bands centred at 740 and 800 nm can be identified with the ${}^4I_{9/2} \rightarrow {}^4F_{7/2},{}^4S_{3/2}$ and ${}^4I_{9/2} \rightarrow {}^4F_{5/2},{}^2H_{9/2}$ transitions of Nd^{3+} ions [4].

Fig. 2 shows the different excitation and emission bands detected at room temperature in the range 200–1450 nm. In this figure, the emission spectra are symbolised by continuous lines while their corresponding excitation bands are represented by dotted lines.

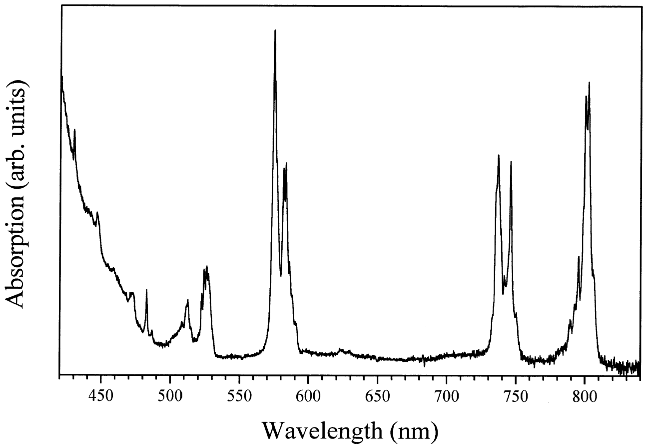

Fig. 1. Optical absorption spectra at liquid helium temperature of the natural fluorapatite in the 420–840 nm spectral region. Most of the absorption bands can be assigned to Nd^{3+} ions.

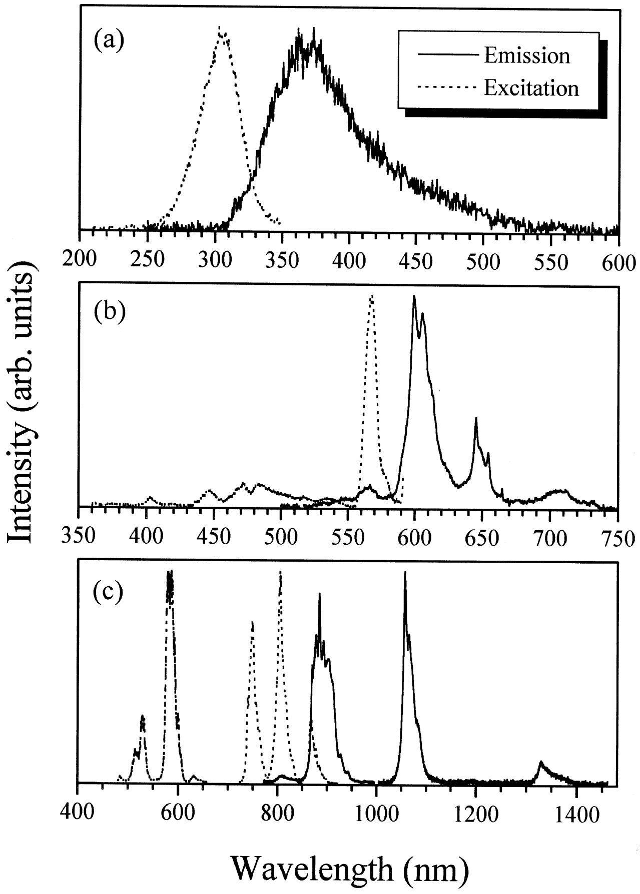

Fig. 2. Emission and excitation spectra, continuous and dotted line, respectively, associated to the presence of several rare-earth impurities in the fluorapatite crystals: (a) Ce^{3+}, (b) Pr^{3+} and (c) Nd^{3+} ions.

When the excitation is performed in the ultraviolet range (Fig. 2a), 250–350 nm spectral region, a wide emission band from 300 to 550 nm can be detected. This broad emission band is similar to that observed in other synthetic crystals doped with Ce^{3+} ions [5], its origin being related with electronic radiative de-excitations from the $5d^1$ to the $4f^1$ orbitals, corresponding to the $D_{3/2,\,5/2} \rightarrow {}^2F_{7/2,\,5/2}$ cerium transitions.

The most intense visible emission, detected even with the naked eye, is located in the 500–750 nm spectral range (Fig. 2b). This red emission can be widely excited between 400 and 550 nm, although the most intense emission takes place when the excitation is tuned between 550 and 600 nm. The excitation spectrum is energetically coincident with different absorption bands attributed to the presence of Nd^{3+} and Pr^{3+} ions in the crystal lattice [4,6,7]. Nevertheless, in contrast to Nd^{3+} ions, it is known that the red emission of Pr^{3+} ions presents a high quantum efficiency [7], and thus this emission can be attributed to the ${}^1D_2 \rightarrow {}^3H_4$ praseodymium transition. However, the overlapping between the Nd^{3+} and Pr^{3+} absorption bands in the visible region could open new de-excitation channels, in particular energy transfer mechanisms, that would affect the dynamical aspects of the red emission.

Fig. 2c shows the emission/excitation bands in the near infrared spectral region (790–1450 nm). These emission/excitation spectra are characteristic of Nd^{3+} ions [4]. In particular, the three main emission bands detected centred at 900, 1060 and 1330 nm, correspond to the radiative relaxation from the $^4F_{3/2}$ excited state to the $^4I_{9/2}$, $^4I_{11/2}$ and $^4I_{13/2}$ neodymium lower lying levels [4].

The dynamic aspects of the different emissions have been investigated under pulsed excitation at 575 nm, in order to corroborate the presence of energy transfer mechanisms between the Pr^{3+} and Nd^{3+} ions. Fig. 3 shows the temporal evolution of the dominant emissions at 600, 900, 1056 and 1330 nm.

The temporal decay of the red emission, centred at 600 nm (circles), presents a fast component followed by a slower decay. This is the typical signature which lets the energy transfer processes act as additional de-excitation channels. The lifetime behaviour indicates that in the first stage ($t<100$ μs), the relaxation of the donor ions is governed by the energy transfer to the acceptor ions.

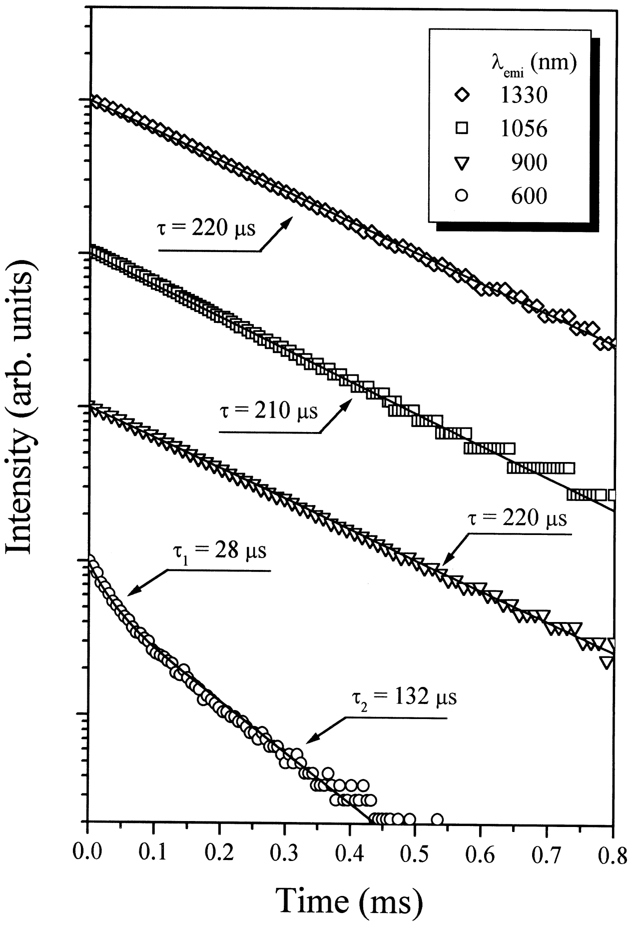

Fig. 3. Lifetime measurements corresponding to the emissions centred at 1330 (diamonds), 1056 (squares), 900 (triangles) and 600 nm (circles) associated, respectively, to the $^4F_{3/2}\rightarrow{}^4I_{9/2}$ (Nd^{3+}), $^4F_{3/2}\rightarrow{}^4I_{11/2}$ (Nd^{3+}), $^4F_{3/2}\rightarrow{}^4I_{13/2}$ (Nd^{3+}) and $^1D_2\rightarrow{}^3H_4$ (Pr^{3+}) transitions.

On the other hand, and assuming that the back-transfer processes are also possible, the acceptor ions can also relax by the inverse energy transfer process which would generate the excitation of the donor ions. Thus as it has been observed in other co-doped crystals [8,9], in the second stage the transfer and back-transfer processes reach a dynamical equilibrium and therefore a parallel evolution of the population in the donor and acceptor levels takes place. In contrast to the first stage, now temporal evolution is dominated by the radiative and non-radiative transitions while the role of the energy transfer processes is to maintain a constant population ratio between both levels. As a consequence of the interaction between the donor and acceptor levels a slower decay is observed in this stage.

Thus, the temporal evolution of the red emission indicates that after 100 μs the transfer and back-transfer processes are equilibrated and the donor and acceptor levels present a parallel decay which can be described with a lifetime value around 132 μs.

The infrared emissions (diamonds, squares and down triangles corresponding to 1330, 1056 and 900 nm, respectively) present a single exponential decay which in all cases can be fitted with similar values of the lifetime. Taking into account that all these emissions arise from the radiative de-excitation of the $^4F_{3/2}$ neodymium excited manifold to the lower lying levels ($^4I_{9/2}$, $^4I_{11/2}$ and $^4I_{13/2}$), the lifetime of this level in the natural fluorapatites investigated is 215 μs with an error, $\Delta\tau/\tau$, close to 2%. This lifetime value is similar to that reported for this level in solid state lasers based on Nd^{3+} ions [10], indicating that it would be possible to achieve laser action in this natural crystal.

4. Conclusion

Natural fluorapatites have been investigated by means of optical absorption, photoluminescence and lifetimes. These spectroscopic tools have allowed to detect several impurities in the lattice, in particular trivalent rare-earth ions such as Ce^{3+}, Nd^{3+} and Pr^{3+} have been identified. The temporal decay of the dominant emission bands indicates that energy transfer processes are acting as new de-excitation channels between the Nd^{3+} and Pr^{3+} ions. In addition, the lifetime of the neodymium metastable level ($^4F_{3/2}$) is similar to that reported for other Nd^{3+}-activated solid state laser materials.

Acknowledgements

Work partially supported by DGES Ministerio de Educación y Cultura (PB97-0019) and Comunidad de Madrid (07T/0026/1998).

References

[1] K.B. Steinbruegge, T. Henningsen, R.H. Hopkins, R. Mazelsky, N.T. Melamet, E. Riedel, G.W. Roland, Appl. Opt. 11 (1972) 999.

[2] G. Lifante, T. Calderón, Bol. Soc. Esp. Mineralogía 13 (1990) 109.

[3] C. Knutson, D.R. Peacar, W.C. Kelly, Am. Mineral. 70 (1985) 829.

[4] A. Brenier, G. Boulon, J. Lumin. 82 (1999) 285.

[5] R.G. Pappalardo, J. Walsh, R.B. Hunt, J. Electrochem. Soc. 130 (1983) 2087.

[6] I. Baumann, F. Cussó, B. Herreros, H. Holzbrecher, H. Paulus, K. Schäfer, W. Sohler, Appl. Phys. A 68 (1999) 321.

[7] B. Savoini, J.E. Muñoz Santiuste, R. González, Phys. Rev. B 56 (1997) 5856.

[8] E. Cantelar, F. Cussó, Appl. Phys. B 29 (1999) 29.

[9] E. Cantelar, F. Cussó, J. Phys.: Condens. Matter 12 (2000) 521.

[10] G. Lifante, F. Cussó, F. Jaque, J.A. Sanz-García, A. Monteil, B. Varrel, G. Boulon, J. García-Solé, Chem. Phys. Lett. 176 (1991) 482.